Drought, agricultural adaptation, and sociopolitical collapse in the Maya Lowlands

Peter M. J. Douglas[a,1,2], Mark Pagani[a], Marcello A. Canuto[b], Mark Brenner[c], David A. Hodell[d], Timothy I. Eglinton[e,f], and Jason H. Curtis[c]

[a]Department of Geology and Geophysics, Yale University, New Haven, CT 06520; [b]Middle American Research Institute, Tulane University, New Orleans, LA 70118; [c]Department of Geological Sciences & Land Use and Environmental Change Institute, University of Florida, Gainesville, FL 32611; [d]Godwin Laboratory for Paleoclimate Research, Department of Earth Sciences, Cambridge University, Cambridge CB2 3EQ, United Kingdom; [e]Department of Marine Chemistry and Geochemistry, Woods Hole Oceanographic Institution, Woods Hole, MA 02543; and [f]Geological Institute, ETH Zurich, 8092 Zurich, Switzerland

Edited by B. L. Turner, Arizona State University, Tempe, AZ, and approved March 20, 2015 (received for review October 3, 2014)

Paleoclimate records indicate a series of severe droughts was associated with societal collapse of the Classic Maya during the Terminal Classic period (~800–950 C.E.). Evidence for drought largely derives from the drier, less populated northern Maya Lowlands but does not explain more pronounced and earlier societal disruption in the relatively humid southern Maya Lowlands. Here we apply hydrogen and carbon isotope compositions of plant wax lipids in two lake sediment cores to assess changes in water availability and land use in both the northern and southern Maya lowlands. We show that relatively more intense drying occurred in the southern lowlands than in the northern lowlands during the Terminal Classic period, consistent with earlier and more persistent societal decline in the south. Our results also indicate a period of substantial drying in the southern Maya Lowlands from ~200 C.E. to 500 C.E., during the Terminal Preclassic and Early Classic periods. Plant wax carbon isotope records indicate a decline in C_4 plants in both lake catchments during the Early Classic period, interpreted to reflect a shift from extensive agriculture to intensive, water-conservative maize cultivation that was motivated by a drying climate. Our results imply that agricultural adaptations developed in response to earlier droughts were initially successful, but failed under the more severe droughts of the Terminal Classic period.

Maya civilization | drought | societal collapse | climate adaptation | compound-specific isotope analysis

The decline of the lowland Classic Maya during the Terminal Classic period (800–900/1000 C.E.) is a preeminent example of societal collapse (1), but its causes have been vigorously debated (2–5). Paleoclimate inferences from lake sediment and cave deposits (6–11) indicate that the Terminal Classic was marked by a series of major droughts, suggesting that climate change destabilized lowland Maya society. Most evidence for drought during the Terminal Classic comes from the northern Maya Lowlands (Fig. 1) (6–8, 10), where societal disruption was less severe than in the southern Maya Lowlands (12, 13). There are fewer paleoclimate records from the southern Maya Lowlands, and they are equivocal with respect to the relative magnitude of drought impacts during the Terminal Classic (9, 11, 14). Further, the supposition that hydrological impacts were a primary cause for societal change is often challenged by archaeologists, who stress spatial variability in societal disruption across the region and the complexity of human responses to environmental change (2, 3, 12). The available paleoclimate data, however, do not constrain possible spatial variability in drought impacts (6–11). Arguments for drought as a principal cause for societal collapse have also not considered the potential resilience of the ancient Maya during earlier intervals of climate change (15).

For this study, we analyzed coupled proxy records of climate change and ancient land use derived from stable hydrogen and carbon isotope analyses of higher-plant leaf wax lipids (long-chain *n*-alkanoic acids) in sediment cores from Lakes Chichancanab and Salpeten, in the northern and southern Maya Lowlands, respectively (Fig. 1). Hydrogen isotope compositions of *n*-alkanoic acids (δD_{wax}) are primarily influenced by the isotopic composition of precipitation and isotopic fractionation associated with evapotranspiration (16). In the modern Maya Lowlands, δD_{wax} is well correlated with precipitation amount and varies by 60‰ across an annual precipitation gradient of 2,500 mm (Fig. 2). This modern variability in δD_{wax} is strongly influenced by soil water evaporation (17), and it is possible that changes in potential evapotranspiration could also impact paleo records. Accordingly, we interpret δD_{wax} values as qualitative records of water availability influenced by both precipitation amount and potential evapotranspiration. These two effects are complementary, since less rainfall and increased evapotranspiration would lead to both increased δD_{wax} values and reduced water resources, and vice versa.

Plant wax carbon isotope signatures ($\delta^{13}C_{wax}$) in sediments from low-elevation tropical environments, including the Maya lowlands, are primarily controlled by the relative abundance of C_3 and C_4 plants (18–20). Ancient Maya land use was the dominant influence on the relative abundance of C_3 and C_4 plants during the late Holocene, because Maya farmers cleared C_3 plant-dominated forests and promoted C_4 grasses, in particular, maize (21–24). Thus, we apply $\delta^{13}C_{wax}$ records as an indicator of the relative abundance of C_4 and C_3 plants that reflects past land use change (*SI Text*). Physiological differences between plant groups also result in differing δD_{wax} values between C_3 trees and shrubs and C_4 grasses (16), and we use $\delta^{13}C_{wax}$ records to correct for the influence of vegetation change on δD_{wax} values (25) ($\delta D_{wax\text{-}corr}$, *SI Text* and Fig. S1).

Significance

The Terminal Classic decline of the Maya civilization represents a key example of ancient societal collapse that may have been caused by climate change, but there are inconsistencies between paleoclimate and archaeological evidence regarding the spatial distribution of droughts and sociopolitical disintegration. We conducted a new analysis of regional drought intensity that shows drought was most severe in the region with the strongest societal collapse. We also found that an earlier drought interval coincided with agricultural intensification, suggesting that the ancient Maya adapted to previous episodes of climate drying, but could not cope with the more extreme droughts of the Terminal Classic.

Author contributions: P.M.J.D. and M.P. designed research; P.M.J.D. performed research; T.I.E. contributed new reagents/analytic tools; P.M.J.D., M.P., M.A.C., M.B., D.A.H., and J.H.C. analyzed data; and P.M.J.D., M.P., M.A.C., and M.B. wrote the paper.

The authors declare no conflict of interest.

This article is a PNAS Direct Submission.

[1]Present address: Division of Geological and Planetary Sciences, California Institute of Technology, Pasadena, CA 91125.

[2]To whom correspondence should be addressed. Email: pdouglas@caltech.edu.

This article contains supporting information online at www.pnas.org/lookup/suppl/doi:10.1073/pnas.1419133112/-/DCSupplemental.

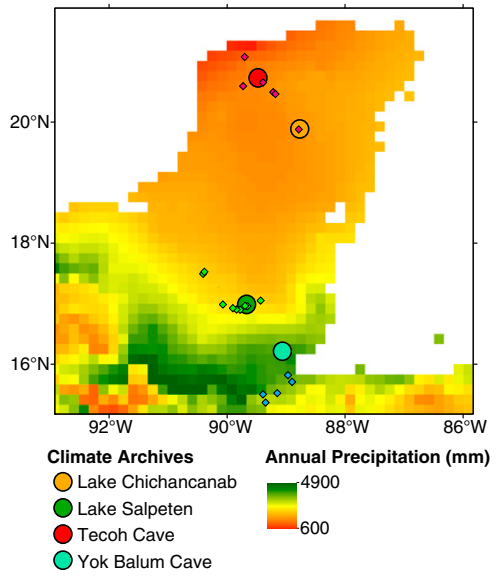

Fig. 1. Map of the Maya Lowlands indicating the distribution of annual precipitation (64) and the location of paleoclimate archives discussed in the text. The locations of modern lake sediment and soil samples (Fig. 2) are indicated by diamonds.

Plant waxes have been shown to have long residence times in soils in the Maya Lowlands (26). Therefore, age–depth models for our plant wax isotope records are based on compound-specific radiocarbon ages (Fig. 3), which align our δD_{wax} records temporally with nearby hydroclimate records derived from other methodologies (26) (*SI Text* and Fig. S2). The mean 95% confidence range for the compound-specific age–depth models is 230 y at Lake Chichancanab and 250 y at Lake Salpeten. Given these age uncertainties, we focus our interpretation on centennial-scale variability (26). The temporal resolution of our plant wax isotope records is lower than speleothem-derived climate records (8, 9), but combining plant wax records from multiple sites allows comparisons of climate change and land use in the northern and southern Maya Lowlands, which would otherwise not be possible. In addition, plant wax isotope records extend to the Early Preclassic/Late Archaic period (1500–2000 B.C.E.), providing a longer perspective on climate change in the Maya Lowlands than most other regional records (6, 8–11).

Results and Discussion

Intersite Comparison of $\delta D_{wax\text{-}corr}$ Hydroclimate Records. A key strength of δD_{wax} in the Maya Lowlands is the well-defined spatial relationship between sedimentary δD_{wax} and annual precipitation amount in this region (Fig. 2). Evaporative enrichment of soil-water D/H ratios—primarily associated with annual precipitation amount—is thought to be the dominant mechanism for the spatial range in δD_{wax} in the Maya Lowlands (17), while other climate variables explain much less of the variability in δD_{wax} (Fig. S3). In particular, potential evapotranspiration (PET), which can also influence soil–water D/H ratios, varies much less than annual precipitation and has a much lower correlation with δD_{wax} values (Fig. S3). Application of a vegetation correction to δD_{wax} values in modern lake sediments and soils ($\delta D_{wax\text{-}corr}$; *SI Text*) to account for differences in the apparent D/H fractionation between environmental water and plant waxes in different plant groups (25) improves its correlation with annual precipitation. Residual variance in $\delta D_{wax\text{-}corr}$ values from lake surface sediments and topsoils, on the order of ±10‰ (Fig. 2), could result from site-specific differences in edaphic properties or microclimates that influence evapotranspiration. It is also possible that the incorporation of aged, soil-derived plant waxes into lake surface sediments contributes to scatter in $\delta D_{wax\text{-}corr}$ values, although this process would not influence topsoil samples (26), or that the applied vegetation correction does not fully account for δD_{wax} differences between plant groups. Importantly, $\delta D_{wax\text{-}corr}$ values in surface sediments from Lakes Chichancanab and Salpeten are within error of the mean value for their respective regions, implying that $\delta D_{wax\text{-}corr}$ values at these lakes are not strongly influenced by nonclimatic factors. Accordingly, differences in $\delta D_{wax\text{-}corr}$ values between these two lake sediment cores can be used as an indicator of spatial differences in hydroclimate in the Maya Lowlands.

Past variability in $\delta D_{wax\text{-}corr}$ reflects the combined effects of evaporative enrichment of soil and plant water D/H ratios and temporal variability in the isotopic composition of precipitation, which, in this region, is primarily controlled by the amount effect (8, 27). Past variability in the evaporative enrichment of soil–water D/H ratios could be influenced by changes in both precipitation amount and PET. Temperature is the dominant influence on PET (28), however, and we assume, based on paleotemperature estimates, that both temperature and PET remained relatively constant in this region during the late Holocene (29). Regardless, if PET did vary, it would have impacted ancient Maya water resources by altering the evaporation of soil moisture and water storage reservoirs, and therefore we interpret $\delta D_{wax\text{-}corr}$ values as a qualitative indicator of past water availability. It is also possible that the strength of the amount effect varied between the northern and southern Maya Lowlands, which would lead to differential changes in $\delta D_{wax\text{-}corr}$ in these two regions for a given decrease in rainfall amount. However, the two Global Network of Isotopes in Precipitation stations nearest to the Maya Lowlands (i.e., Veracruz, Mexico and San Salvador, El Salvador) record nearly identical $\delta^{18}O$ precipitation amount slopes (27) and thus suggest that the strength of the amount effect is largely invariant across southern Mexico and Central America.

In contrast to $\delta D_{wax\text{-}corr}$ records, $\delta^{18}O$ values in carbonate shells from lake sediments and in cave carbonate can be strongly impacted by nonclimatic factors that influence local hydrology or $^{18}O/^{16}O$ fractionation between water and carbonate (14, 30–32).

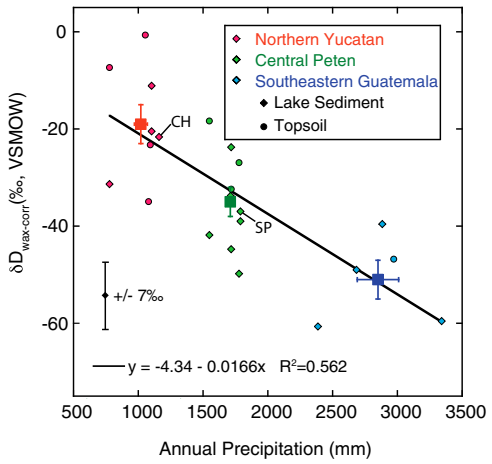

Fig. 2. Scatter plot showing the negative relationship between annual precipitation and $\delta D_{wax\text{-}corr}$ measured in modern lake sediment and soil samples (Fig. 1). Results from Lake Chichancanab (CH) and Salpeten (SP) are indicated. The black line indicates a linear regression fit to these data, with regression statistics reported at the bottom of the plot. Large squares indicate mean values for each sampling region, with error bars indicating SEM in both $\delta D_{wax\text{-}corr}$ and annual precipitation. The black error bar indicates the 1σ error for $\delta D_{wax\text{-}corr}$ values (*SI Text*). Original δD_{wax} data from ref. 17. VSMOW, Vienna Standard Mean Ocean Water.

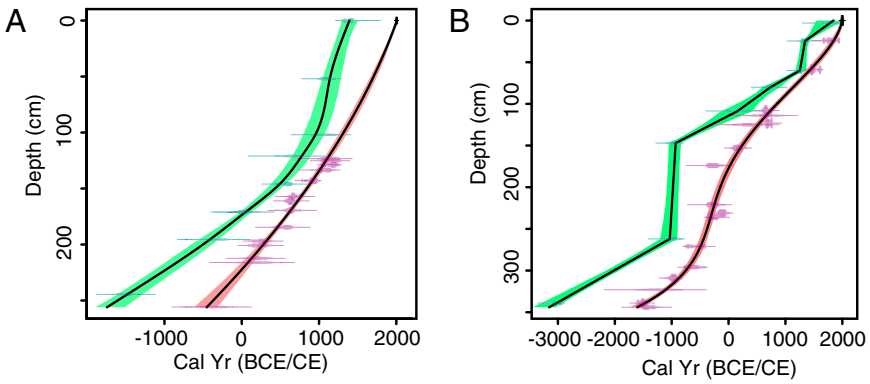

Fig. 3. Plant wax (green; left) and terrigenous macrofossil (red; right) age–depth models for (*A*) Lake Chichancanab and (*B*) Lake Salpeten. The age probability density of individual radiocarbon analyses is shown. The black lines indicate the best age model based on the weighted mean of 1,000 age model iterations (62). Colored envelopes indicate 95% confidence intervals. Cal, calendar.

Thus, although carbonate $\delta^{18}O$ values within an individual lake sediment core or cave speleothem typically provide a robust indicator of past climate change at a given site, these data cannot be readily compared between lakes or caves to determine spatial differences in climatic change. Notably, modern $\delta^{18}O$ values for the Yok I speleothem in southern Belize (~−3.4‰) are ^{18}O-enriched relative to modern $\delta^{18}O$ values for the Chaac speleothem in the northern Yucatan (~−5.4‰) (Fig. 4*B*). This isotopic difference is unexpected, given the much wetter climate at Yok Balum Cave and relatively small differences in the isotopic composition of precipitation across the region (17). The difference in $\delta^{18}O$ between the two sites is likely the result of combined evaporative and kinetic isotope effects that influence the Yok I record (9), although these isotopic offsets have not been thoroughly examined. As a consequence, comparison of speleothem isotope records does not provide a clear indication of spatial variability in past climate change in the Maya Lowlands. Similar site-specific hydrological influences confound spatial comparisons between lake sediment $\delta^{18}O$ records (14, 33). Therefore, comparative analysis of $\delta D_{wax\text{-}corr}$ records from Lake Chichancanab and Lake Salpeten provide a unique and powerful tool for understanding how hydrological variability across the region impacted the ancient Maya.

Patterns of Hydroclimate Change in the Maya Lowlands. Our results from Lakes Chichancanab and Salpeten confirm the occurrence of severe and extended droughts throughout the Maya Lowlands during the Terminal Classic (Fig. 4*A*), with the magnitude of $\delta D_{wax\text{-}corr}$ change (~50–60‰) equivalent to the modern range in $\delta D_{wax\text{-}corr}$ from northern Yucatan to southeastern Guatemala (where annual precipitation ranges from 800 mm to 3,300 mm; Fig. 2). Indeed, major droughts inferred from $\delta D_{wax\text{-}corr}$ during the Terminal Classic represent the driest regional conditions of the preceding ~1,200 y at Lake Chichancanab and of the preceding ~2,500 y at Lake Salpeten. Importantly, our $\delta D_{wax\text{-}corr}$ records further imply that the large, modern precipitation gradient between Lake Chichancanab and Lake Salpeten (~550 mm; Fig. 1) changed significantly over time (Fig. 5) and that the hydrologic differences between the northern and southern Maya Lowlands effectively disappeared during the Terminal Classic (Fig. 5), with substantially greater drying in the southern lowlands relative to the northern lowlands (Fig. 4).

Differential patterns of paleohydroclimate change between these two sites are consistent with analyses of 20th-century rainfall variability that show poor correlation between the northern Yucatan Peninsula and the southern lowlands south of 17°N (8). Mechanistic explanations for these differences remain unresolved, but two scenarios are plausible. Today, the relatively dry climate of northern Yucatan (Fig. 1) results from atmospheric subsidence related to the descending limb of the Hadley cell (34). A southward shift of the Hadley cell during the Terminal Classic (9, 35) would have caused the region of subsidence to expand to the south, and could have led to a stronger decrease in precipitation in the southern lowlands relative to the northern lowlands.

Alternatively, different sensitivities to past ocean circulation could have played a role. Interoceanic temperature gradients between the tropical Atlantic and the eastern tropical Pacific are an important driver of summer rainfall variability in Central America (36, 37), and paleoclimate studies have found evidence for a Pacific influence on hydroclimate in northern Guatemala and other regions of Mesoamerica (38–40). In contrast, recent variability in precipitation across northern Yucatan does not appear to have a consistent relationship with Pacific climate variability (36, 41, 42).

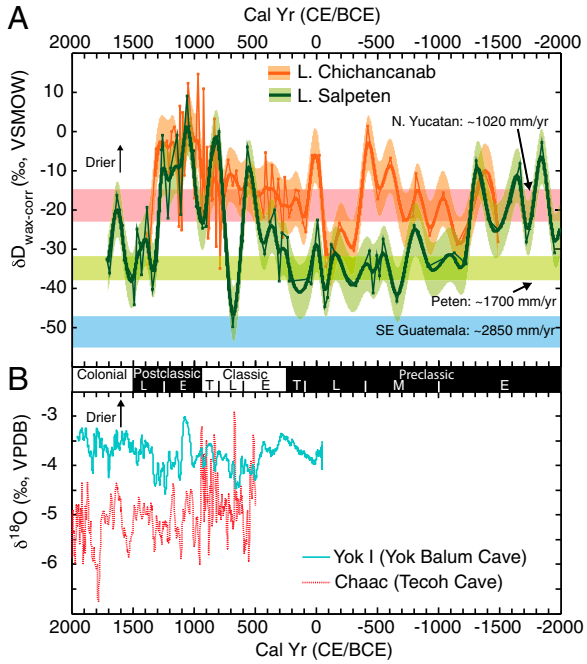

Fig. 4. (*A*) The $\delta D_{wax\text{-}corr}$ records from Lakes Chichancanab and Salpeten, fit with a smoothing spline (thicker lines) to highlight centennial-scale trends. Colored envelopes indicate 1σ error in $\delta D_{wax\text{-}corr}$ values (±7‰) applied to the smoothing spline fits. Horizontal bands indicate the mean $\delta D_{wax\text{-}corr}$ values for lake surface sediments and soils from three regions within the Maya Lowlands with different mean annual precipitation (Fig. 2); the width of the bands indicates the SEM of regional mean values. (*B*) The $\delta^{18}O$ records from two speleothems from the northern (Chaac) and southern (Yok I) Maya Lowlands (8, 9) (Fig. 1), plotted on a common scale to highlight differences in the range and amplitude of $\delta^{18}O$ variability for these two records. E, Early; M, Middle; L, Late; T, Terminal; VPDB, Vienna Pee Dee Belemnite.

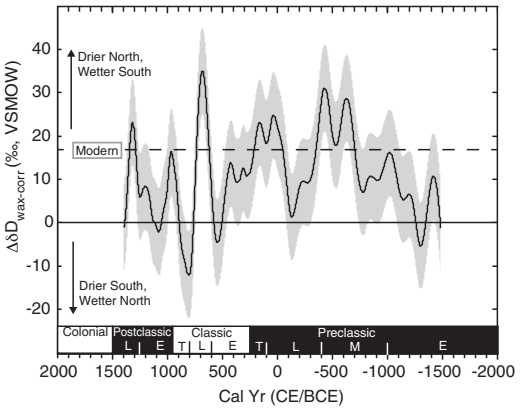

Fig. 5. Record of the difference in δD_{wax} ($\Delta\delta D_{wax}$) between Lake Chichancanab and Lake Salpeten, indicating changes in the precipitation gradient between the northern and southern Maya Lowlands. $\Delta\delta D_{wax}$ is calculated as the difference between smoothing spline curves fit to isotopic data from each lake core (Fig. 3). The gray envelope indicates the propagated 1σ error for $\Delta\delta D_{wax}$ (±10‰). Modern $\Delta\delta D_{wax}$ (Fig. 2) is indicated by the dashed line.

Rather, past hydroclimate variability in northern Yucatan appears to be primarily linked to the climate of the North Atlantic (10, 43) and may be influenced by North Atlantic tropical cyclones (44). Paleoclimate data indicate increased El Niño event frequency between ~250 C.E. and 1400 C.E. (45), coinciding with drier and more variable hydroclimate at Lake Salpeten (Fig. 4). We suggest that this change in Pacific climate could have increased drought frequency in the southern Maya lowlands by reducing Atlantic–Pacific temperature gradients, but had a lesser impact in the northern Maya lowlands.

Climate Change and Sociopolitical Responses. Changes in hydrological conditions and sociopolitical evolution appear to be linked on centennial timescales in the southern Maya Lowlands. Our Lake Salpeten $\delta D_{wax\text{-}corr}$ record suggests that the southern Lowlands experienced relatively wet and stable conditions during much of the Middle and Late Preclassic periods (~700 B.C.E. to 200 C.E.)—times marked by continuous demographic growth and increasing sociopolitical complexity throughout the region. The Middle Preclassic gave rise to the first cities with concentrated populations, writing, and public monuments (46, 47), followed by the rise of hierarchical and centralized states during the Late Preclassic period (48).

Lake Salpeten $\delta D_{wax\text{-}corr}$ values indicate pronounced drying from ~200 C.E. to 500 C.E., a pattern that is broadly consistent with other hydroclimate records from the southern Maya Lowlands (9, 11, 14). Drying during the Early Classic period is associated with the decline and abandonment of some of the largest Late Preclassic political systems in the third century C.E. and subsequent political fragmentation in the region (15, 46). During that time, widespread political realignment developed gradually under the strong influence of a foreign power, the central Mexican city of Teotihuacan (49). We suggest that climatological stress disrupted the largest Late Preclassic states, enabling smaller and more resilient polities to grow by using adaptations to more variable conditions, such as water conservation (50).

A negative 35‰ δD shift at the beginning of the Late Classic period (~600 C.E.) indicates substantially wetter conditions around Lake Salpeten for almost two centuries that coincided with a period of intense architectural construction, political expansion, and resource consumption throughout the southern lowlands, including the rise and expansion of large, centralized political entities such as Calakmul and Tikal (51, 52). Dry conditions returned to the southern lowlands around the beginning of the Terminal Classic period (~800 C.E.), intensified during the early Postclassic period, and ended *ca.* 1300 C.E. During this time, political complexity in the southern Maya Lowlands underwent a fitful but inexorable regional decline (3). Monument building and written inscriptions essentially ceased after 820 C.E., and the institution of centralized kingship—the main organizing entity of the southern lowlands throughout the first millennium C.E.—disappeared forever (5, 53, 54). Importantly, political decline in the southern lowlands during the Terminal Classic differed from that at the end of the Preclassic period in that it was not followed by the development of new, resilient political centers. We argue that the absence of a significant Postclassic recovery in the southern lowlands was related to the more intense and sustained interval of drought in the region.

Ancient Maya Land Use Change and Climate Adaptation. Ancient lowland Maya populations adapted to available water resources and used a diverse set of land use practices (13, 55) that likely preconditioned their vulnerability to hydrological change. Whereas $\delta D_{wax\text{-}corr}$ reflects hydrological conditions, $\delta^{13}C_{wax}$ records reflect the relative proportion of C_3 and C_4 plants in the lake catchment, and thus local agricultural practices (*SI Text*). During the Preclassic period, C_4 plant abundance in both the Lake Salpeten and Lake Chichancanab catchments was relatively high, with large variability on centennial timescales (Fig. 6 *A* and *B*). A long-term shift toward fewer C_4 plants occurred at the beginning of the Classic period in both catchments. Relatively low C_4 plant abundance persisted in both catchments into the Early Postclassic, followed by an increase at the end of that period. The inferred decrease in C_4 plant coverage at Lake Salpeten is

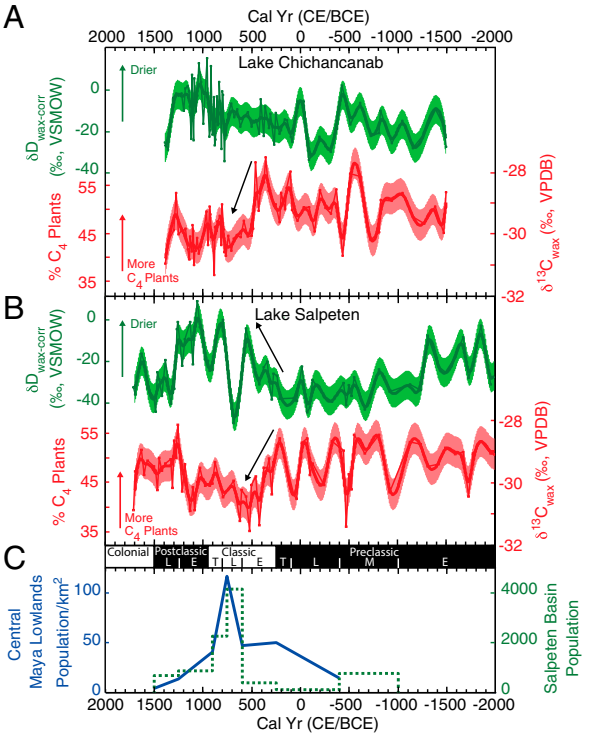

Fig. 6. Coupled plant wax isotope records of hydroclimate and land use change from (*A*) Lake Chichancanab and (*B*) Lake Salpeten, alongside (*C*) estimates of population in the Lake Salpeten catchment (56) and population density in the central portion of the southern Maya Lowlands (57). The $\delta D_{wax\text{-}corr}$ and $\delta^{13}C_{wax}$ records in *A* and *B* are fit to a smoothing spline (thicker lines) to highlight centennial-scale trends. Colored envelopes indicate 1σ error applied to the smoothing spline fits for $\delta D_{wax\text{-}corr}$ (±7‰) and $\delta^{13}C_{wax}$ (±0.5‰). Estimates of percent C_4 plants are discussed in *SI Text*.

consistent with pollen records that show decreased grass abundance in the Early Classic period (21) (Fig. S4 and *SI Text*), accompanied by an increase in C_3 plant disturbance taxa (Fig. S4).

The Early Classic trend of decreasing C_4 plant abundance in these two catchments directly coincides with drying trends in both the northern and southern Maya lowlands (Fig. 6 *A* and *B*), as well evidence of population growth both locally at Lake Salpeten (56) and across the southern Maya Lowlands regionally (57) (Fig. 6*C*) during the Classic period. Consequently, it is unlikely that evidence for fewer C_4 plants reflects a regional reduction in maize agriculture. Instead, we argue that increasingly negative $\delta^{13}C_{wax}$ trends mark adaptations of local land use in response to drier conditions. In both lake catchments, the Preclassic period was likely characterized by widespread application of rain-fed swidden (slash-and-burn) agriculture that promoted maize and other C_4 plant growth. The drier conditions during the Early Classic period would have inhibited swidden agriculture. Geoarchaeological evidence suggests that intensive agricultural strategies were adopted during the Classic period in many areas of the Maya Lowlands (55, 58, 59), possibly in response to limited rainfall (58). We suggest that the growth of population around Lake Salpeten was associated with a reduction in swidden agriculture and its replacement by increased intensive maize cultivation outside the lake catchment in places with reliable water resources, including seasonal and perennial wetlands (58, 59). If local land use changes in our two studied sites were representative of broader patterns, they imply a shift to spatially concentrated and regionally integrated agricultural economies during the Early Classic period that encouraged the growth of high-density population centers.

Given the Classic period population growth surrounding Lake Salpeten, it appears that such adaptations were an effective response to the drier conditions of the Early Classic period. Further, with the onset of wetter conditions in the Late Classic period, these agricultural strategies would have promoted enhanced population growth and agricultural productivity, contributing to increased sociopolitical centralization and expansion. By increasing societal complexity, however, the organization of lowland Classic Maya society into large, centralized states could have reduced resilience to the more intense droughts of the Terminal Classic (1).

Conclusions

Carbon and hydrogen isotope compositions of sedimentary plant waxes from Lakes Chichancanab and Salpeten support the hypothesis that drought was instrumental to the Terminal Classic decline of the Classic Maya throughout the Maya Lowlands. Drying was more intense in the southern lowlands, where societal collapse occurred earliest and was most pronounced and permanent. Our work further suggests that the Maya successfully adapted land use practices during previous droughts of the Early Classic period, but that more severe droughts during the Terminal Classic, as well as the increased complexity of Late Classic societies, made adaptation to climate change less effective.

Materials and Methods

Sediment Cores and Sampling. Lake Chichancanab is an elongate, fault-bounded karst lake located in the interior of the Yucatan Peninsula, Mexico (Fig. 1). The sediment core we analyzed was collected with a piston corer in 14.5 m of water, in March 2004 (6). Lake Chichancanab sediments are composed primarily of low-density organic-rich gyttja, but possess distinctive intervals of high-density gypsum, deposited during periods of drought (6). The δD_{wax} data from this core were reported in ref. 26; high-resolution $\delta^{13}C_{wax}$ data from this core are presented here for the first time, to our knowledge.

Lake Salpeten is one of a series of east–west aligned lakes in central Petén, northern Guatemala. The Lake Salpeten sediment core was collected with a piston corer in 16 m of water, in August 1999 (14). Uppermost and lowermost sediments from Lake Salpeten are organic-rich gyttja, whereas the central portion of the core is composed of dense clay, thought to be the result of intense soil erosion caused by ancient Maya land clearance (14). This contrasts with Lake Chichancanab, where there is no sedimentological evidence for large-scale soil erosion.

Plant Wax Lipid Extraction and Preparation. Methods for plant wax lipid extraction and preparation were previously described (26). Briefly, all sediment core samples were freeze dried and solvent extracted. Between 0.5 g and 23 g of dry sediment were extracted per sample. The total lipid extract was then hydrolyzed, and acid and neutral fractions were extracted.

The acid fraction of all samples was esterified using 14% boron trifluoride in methanol. The resulting fatty acid methyl esters (FAMEs) were then purified using silica gel chromatography. Purified FAMEs were quantified relative to an external quantitative standard by gas chromatography.

Compound-Specific Stable Isotope Analyses. Methods for plant wax stable isotope analyses were previously described (26). The δD and $\delta^{13}C$ values for individual FAMEs were determined by gas chromatography isotope ratio mass spectrometry (GC-IRMS) at the Yale University Earth System Center for Stable Isotopic Studies. The H_3^+ factor for the GC-IRMS was measured daily before δD analysis. External and internal FAME isotope standards were used to standardize and normalize sample isotope values. The precision of the standard analyses was $\leq\pm5‰$ for δD analyses and $\leq\pm0.5‰$ for $\delta^{13}C$ analyses. Most samples were run in duplicate or triplicate for both hydrogen and carbon isotope analysis, and the reported isotope ratio value is the mean of replicate runs. For some samples, long-chain FAME abundances were insufficient for replicate analyses. FAME $\delta^{13}C$ and δD values were corrected for the isotopic composition of the methyl group added during esterification, by measuring a phthalic acid standard of known isotopic composition esterified in the same manner as the samples. The δD_{wax} and $\delta^{13}C_{wax}$ values were calculated as the unweighted mean isotopic composition of the *n*-C_{26}, *n*-C_{28}, and *n*-C_{30} alkanoic acid homologs (*SI Text* and Tables S1 and S2).

Compound-Specific Radiocarbon Analyses of Plant Wax Lipids. Methods for plant wax radiocarbon analyses are described in ref. 26. Long-carbon-chain-length FAMEs were isolated using a Preparative Capillary Gas Chromatography system at either the Woods Hole Oceanographic Institution Department of Marine Chemistry and Geochemistry or the National Ocean Sciences Accelerator Mass Spectrometry (NOSAMS) facility (60). Individual FAMES were not sufficiently abundant for $\Delta^{14}C$ analysis, so we combined four long-chain *n*-alkanoic acid homologs (C_{26}, C_{28}, C_{30}, and C_{32}). Isolated FAME fractions were quantified and checked for purity using GC with flame ionization detection. The samples were transferred to precombusted quartz tubes, all solvent was evaporated under nitrogen, and the samples were combusted in the presence of cupric oxide at 850 °C to yield CO_2. The resulting CO_2 was quantified and purified, then reduced to graphite and analyzed for radiocarbon content at the NOSAMS facility. Compound-specific radiocarbon results were corrected for procedural blanks by accounting for the blank contribution determined using the same analytical protocol and equipment (61). A sample of the methanol used for esterification was analyzed for $\Delta^{14}C$ at NOSAMS, and FAME $\Delta^{14}C$ values were corrected for the addition of methyl carbon. $\Delta^{14}C_{wax}$ results from Lake Chichancanab were initially reported in ref. 26; $\Delta^{14}C_{wax}$ results from Lake Salpeten are reported for the first time, to our knowledge, here (Table S3).

Age–Depth Models. The development of terrigenous macrofossil (TM) and plant wax (PW) age–depth models for Lake Chichancanab are described in ref. 26. We used a similar approach to define TM and PW age–depth models for Lake Salpeten. Specifically, we developed a linear-interpolated age–depth PW age model for Lake Salpeten using the Classical Age–depth Modeling (CLAM v2.2) software in R (62). We also recalculated the fourth-order polynomial TM age–depth model for Lake Salpeten (14) using CLAM. All ^{14}C ages were calibrated to calendar ages using the IntCal13 calibration (63).

ACKNOWLEDGMENTS. Gerard Olack, Glendon Hunsinger, and Dominic Colosi provided assistance with compound-specific stable isotope measurements, and Daniel Montluçon, Li Xu, and Ann McNichol provided assistance with compound-specific radiocarbon measurements. Hagit Affek provided helpful comments on an earlier version of the manuscript, and two anonymous reviewers provided constructive commentary. This work was partially funded by the Italian Ministry of the Environment and by a US National Science Foundation Graduate Research Fellowship.

1. Tainter J (1990) *The Collapse of Complex Societies* (Cambridge Univ Press, Cambridge, UK).
2. Aimers JJ (2007) What Maya collapse? Terminal classic variation in the Maya lowlands. *J Archaeol Res* 15(4):329–377.
3. Demarest AA, Rice DS, eds (2005) *The Terminal Classic in the Maya Lowlands: Collapse, Transition, and Transformation* (Univ Press Colorado, Boulder).
4. Iannone G, ed (2014) *The Great Maya Droughts in Cultural Context* (Univ Press Colorado, Boulder).
5. Yaeger J, Hodell DA (2008) The collapse of Maya Civilization: Assessing the interaction of culture, climate, and environment. *El Niño, Catastrophism, and Culture Change*, eds Sandweiss DH, Quilter J (Dumbarton Oaks, Washington, DC), pp 187–242.
6. Hodell DA, Brenner M, Curtis JH (2005) Terminal Classic drought in the northern Maya lowlands inferred from multiple sediment cores in Lake Chichancanab (Mexico). *Quat Sci Rev* 24(12-13):1413–1427.
7. Hodell DA, Curtis JH, Brenner M (1995) Possible role of climate in the collapse of Classic Maya civilization. *Nature* 375(6530):391–394.
8. Medina-Elizalde M, et al. (2010) High resolution stalagmite climate record from the Yucatan Peninsula spanning the Maya terminal classic period. *Earth Planet Sci Lett* 298(1-2):255–262.
9. Kennett DJ, et al. (2012) Development and disintegration of Maya political systems in response to climate change. *Science* 338(6108):788–791.
10. Curtis JH, Hodell DA, Brenner M (1996) Climate variability on the Yucatan Peninsula (Mexico) during the past 3500 years, and implications for Maya cultural evolution. *Quat Res* 46(1):37–47.
11. Webster JW, et al. (2007) Stalagmite evidence from Belize indicating significant droughts at the time of Preclassic Abandonment, the Maya Hiatus, and the Classic Maya collapse. *Palaeogeogr Palaeoclimatol Paleoecol* 250(1-4):1–17.
12. Dahlin BH (2002) Climate change and the end of the Classic Period in Yucatan: Resolving a paradox. *Ancient Mesoam* 13(2):327–340.
13. Turner BL, II, Sabloff JA (2012) Classic Period collapse of the Central Maya Lowlands: Insights about human-environment relationships for sustainability. *Proc Natl Acad Sci USA* 109(35):13908–13914.
14. Rosenmeier MF, Hodell DA, Brenner M, Curtis JH, Guilderson TP (2002) A 4000-year lacustrine record of environmental change in the southern Maya lowlands, Peten, Guatemala. *Quat Res* 57(2):183–190.
15. Dunning N, et al. (2014) The end of the beginning: Drought, environmental change and the Preclassic to Classic transition in the east central Maya Lowlands. *The Great Maya Droughts in Cultural Context: Case Studies in Resilience and Vulnerability*, ed Iannone G (Univ Press Colorado, Boulder), pp 107–126.
16. Sachse D, et al. (2012) Molecular paleohydrology: Interpreting the hydrogen-isotopic composition of lipid biomarkers from photosynthesizing organisms. *Annu Rev Earth Planet Sci* 40:221–249.
17. Douglas PMJ, Pagani M, Brenner M, Hodell DA, Curtis JH (2012) Aridity and vegetation composition are important determinants of leaf-wax δD values in southeastern Mexico and Central America. *Geochim Cosmochim Acta* 97:24–45.
18. Huang Y, et al. (2001) Climate change as the dominant control on glacial-interglacial variations in C_3 and C_4 plant abundance. *Science* 293(5535):1647–1651.
19. Hughen KA, Eglinton TI, Xu L, Makou M (2004) Abrupt tropical vegetation response to rapid climate changes. *Science* 304(5679):1955–1959.
20. Huang YS, Dupont L, Sarnthein M, Hayes JM, Eglinton G (2000) Mapping of C_4 plant input from North West Africa into North East Atlantic sediments. *Geochim Cosmochim Acta* 64(20):3505–3513.
21. Leyden BW (1987) Man and climate in the Maya Lowlands. *Quat Res* 28(3):407–417.
22. Leyden BW (2002) Pollen evidence for climatic variability and cultural disturbance in the Maya lowlands. *Anc Mesoam* 13(1):85–101.
23. Wahl D, Byrne R, Schreiner T, Hansen R (2006) Holocene vegetation change in the northern Peten and its implications for Maya prehistory. *Quat Res* 65(3):380–389.
24. Beach T, et al. (2011) Carbon isotopic ratios of wetland and terrace soil sequences in the Maya Lowlands of Belize and Guatemala. *Catena* 85(2):109–118.
25. Collins JA, et al. (2013) Estimating the hydrogen isotopic composition of past precipitation using leaf-waxes from western Africa. *Quat Sci Rev* 65:88–101.
26. Douglas PMJ, et al. (2014) Pre-aged plant waxes in tropical lake sediments and their influence on the chronology of molecular paleoclimate proxy records. *Geochim Cosmochim Acta* 141:346–364.
27. Lachniet MS, Patterson WP (2009) Oxygen isotope values of precipitation and surface waters in northern Central America (Belize and Guatemala) are dominated by temperature and amount effects. *Earth Planet Sci Lett* 284(3-4):435–446.
28. Rind D, Goldberg R, Hansen J, Rosenzweig C, Ruedy R (1990) Potential evapotranspiration and the likelihood of future drought. *J Geophys Res* 95(D7):9983–10004.
29. Hodell DA, et al. (2012) Late Glacial temperature and precipitation changes in the lowland Neotropics by tandem measurement of $\delta^{18}O$ in biogenic carbonate and gypsum hydration water. *Geochim Cosmochim Acta* 77:352–368.
30. Henderson AK, Shuman BN (2009) Hydrogen and oxygen isotopic compositions of lake water in the western United States. *Geol Soc Am Bull* 121(7-8):1179–1189.
31. Lachniet MS (2009) Climatic and environmental controls on speleothem oxygen-isotope values. *Quat Sci Rev* 28(5):412–432.
32. Kluge T, Affek HP (2012) Quantifying kinetic fractionation in Bunker Cave speleothems using Δ_{47}. *Quat Sci Rev* 49:82–94.
33. Curtis JH, et al. (1998) A multi-proxy study of Holocene environmental change in the Maya lowlands of Peten, Guatemala. *J Paleolimnol* 19(2):139–159.
34. Waliser DE, Shi Z, Lanzante J, Oort A (1999) The Hadley circulation: Assessing NCEP/NCAR reanalysis and sparse in-situ estimates. *Clim Dyn* 15(10):719–735.
35. Haug GH, et al. (2003) Climate and the collapse of Maya civilization. *Science* 299(5613):1731–1735.
36. Giannini A, Kushnir Y, Cane MA (2000) Interannual variability of Caribbean rainfall, ENSO, and the Atlantic Ocean. *J Clim* 13(2):297–311.
37. Taylor MA, Stephenson TS, Owino A, Chen AA, Campbell JD (2011) Tropical gradient influences on Caribbean rainfall. *J Geophys Res* 116(D21)::D00Q08.
38. Lachniet MS, et al. (2004) A 1500-year El Niño/Southern Oscillation and rainfall history for the Isthmus of Panama from speleothem calcite. *J Geophys Res* 109(D20):D20117.
39. Wahl D, Byrne R, Anderson L (2014) An 8700 year paleoclimate reconstruction from the southern Maya lowlands. *Quat Sci Rev* 103:19–25.
40. Stahle D, et al. (2012) Pacific and Atlantic influences on Mesoamerican climate over the past millennium. *Clim Dyn* 39(6):1431–1446.
41. Giddings L, Soto M (2003) Rhythms of precipitation in the Yucatan Peninsula. *The Lowland Maya: Three Millennia at the Human–Wildland Interface*, eds Fedick S, Allen M, Jiminez-Osornio J (Haworth Press, Binghamton, NY), pp 77–90.
42. Pavia EG, Graef F, Reyes J (2006) PDO-ENSO effects in the climate of Mexico. *J Clim* 19(24):6433–6438.
43. Mendoza B, García-Acosta V, Velasco V, Jáuregui E, Díaz-Sandoval R (2007) Frequency and duration of historical droughts from the 16th to the 19th centuries in the Mexican Maya lands, Yucatan Peninsula. *Clim Change* 83(1-2):151–168.
44. Medina-Elizalde M, Rohling EJ (2012) Collapse of Classic Maya civilization related to modest reduction in precipitation. *Science* 335(6071):956–959.
45. Moy CM, Seltzer GO, Rodbell DT, Anderson DM (2002) Variability of El Niño/Southern Oscillation activity at millennial timescales during the Holocene epoch. *Nature* 420(6912):162–165.
46. Hansen RD (2001) The first cities: The beginnings of urbanization and state formation in the Maya Lowlands. *Maya: Divine Kings of the Rainforest*, ed Grube N (Konemann Press, Cologne, Germany), pp 50–65.
47. Estrada-Belli F (2010) *The First Maya Civilization: Ritual and Power Before the Classic Period* (Routledge, London).
48. Hansen RD (2005) Perspectives on Olmec-Maya interaction in the Middle Formative Period. *New Perspectives on Formative Mesoamerican Cultures*, ed Powis TG (Brit Archaeol Rep, Oxford), pp 51–72.
49. Stuart D (2000) Teotihuacan and Tollan in Classic Maya history. *Mesoamerica's Classic Heritage: From Teotihuacan to the Aztecs*, eds Carrasco D, Jones L, Sessions S (Univ Press Colorado, Boulder), pp 465–514.
50. Scarborough VL, et al. (2012) Water and sustainable land use at the ancient tropical city of Tikal, Guatemala. *Proc Natl Acad Sci USA* 109(31):12408–12413.
51. Martin S, Grube N (1995) Maya superstates. *Archaeology* 48(6):41–46.
52. Martin S, Grube N (2008) *Chronicle of the Maya Kings and Queens* (Thames Hudson, London).
53. Webster DL (2002) *The Fall of the Ancient Maya: Solving the Mystery of the Maya Collapse* (Thames Hudson, New York).
54. Demarest AA, Rice PM, Rice DS (2004) The Terminal Classic in the Maya Lowlands: Assessing collapses, terminations, and aftermaths. *The Terminal Classic in the Maya Lowlands: Collapse, Transition, and Transformation* (Univ Press Colorado, Boulder), pp 545–572.
55. Dunning NP, Beach T (2011) Farms and forests: Spatial and temporal perspectives on ancient Maya landscapes. *Landscapes and Societies*, eds Martini IP, Chesworth W (Springer, Dordrecht, The Netherlands), pp 369–389.
56. Rice DS, Rice PM (1990) Population size and population change in the central Peten lakes region, Guatemala. *Precolumbian Population History in the Maya Lowlands*, eds Culbert TP, Rice DS (Univ New Mexico Press, Albuquerque), pp 123–148.
57. Turner BL, II (1990) Population reconstruction of the central Maya Lowlands: 1000 B.C. to A.D. 1500. *Precolumbian Population History in the Maya Lowlands*, eds Culbert TP, Rice DS (Univ New Mexico Press, Albuquerque), pp 301–324.
58. Dunning NP, et al. (2002) Arising from the bajos: The evolution of a neotropical landscape and the rise of Maya civilization. *Ann Assoc Am Geogr* 92(2):267–283.
59. Luzzadder-Beach S, Beach TP, Dunning NP (2012) Wetland fields as mirrors of drought and the Maya abandonment. *Proc Natl Acad Sci USA* 109(10):3646–3651.
60. Eglinton TI, Aluwihare LI, Bauer JE, Druffel ERM, McNichol AP (1996) Gas chromatographic isolation of individual compounds from complex matrices for radiocarbon dating. *Anal Chem* 68(5):904–912.
61. Galy V, Eglinton T (2011) Protracted storage of biospheric carbon in the Ganges-Brahmaputra basin. *Nat Geosci* 4(12):843–847.
62. Blaauw M (2010) Methods and code for 'classical' age-modelling of radiocarbon sequences. *Quat Geochronol* 5(5):512–518.
63. Reimer PJ, et al. (2013) IntCal13 and Marine13 radiocarbon age calibration curves 0–50,000 years cal BP. *Radiocarbon* 55(4):1869–1887.
64. New M, Lister D, Hulme M, Makin I (2002) A high-resolution data set of surface climate over global land areas. *Clim Res* 21(1):1–25.